Lowering the Sensory Threshold and Enhancing the responsivity of Biomimetic Hair Flow Sensors by Electrostatic Spring Softening

Harmen Droogendijk, Christiaan M. Bruinink, Remco G.P. Sanders, Ortwin G. Siebelder and Gijs J.M. Krijnen

MESA+ Research Institute, University of Twente, Enschede, THE NETHERLANDS

E-mail: h.droogendijk@utwente.nl

Abstract—**We report improvements in detection limit and responsivity of biomimetic hair flow sensors by electrostatic spring-softening (ESS). Applying a DC voltage to our capacitive flow sensors results in a reduced sensory threshold, which gives an improvement for the flow detection limit of more than 30%. In addition, the mechanical transfer shows large (80% and more) voltage-controlled electro-mechanical amplification of the flow signal for frequencies below the sensor's resonance.**

I. INTRODUCTION

Nature displays a variety of mechanisms that constitute exceptional sensory performance, e.g. with respect to sensitivity, dynamic range, frequency filtering and selectivity [1], and which forms a rich source of inspiration to engineers. Inspired by crickets and their perception of flow phenomena, artificial hair flow sensors have been developed successfully in our group (Fig. 1) [2]. Improvement of fabrication methodologies has led to better performance, making it possible to detect and measure flow velocities in the range of sub-mm/s [3].
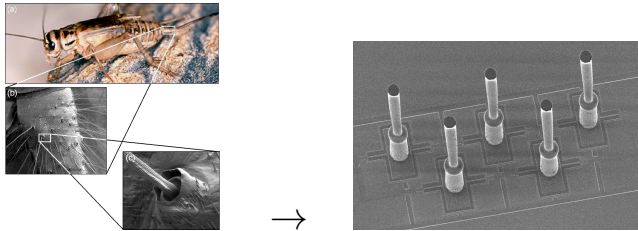

Fig. 1. From flow perception by crickets (SEM pictures courtesy of Jérôme Casas, Université de Tours) to MEMS hair flow sensors fabricated by surface micromachining and using SU-8 lithography.

To increase the sensitivity and enhancing the mechanical transfer of these sensors, we make use of Electrostatic Spring Softening (ESS). Previously, the use of ESS was demonstrated for electrostatically actuated flow sensors [4]. In this work, we show that ESS is indeed applicable to adaptively change the electro-mechanical properties of the system for oscillating air flow perception.

II. THEORY AND MODELING

A. Stiffness control

The motion of a flow susceptible hair is described by a second order mechanical system (Fig. 2) [5], wherein a harmonic air flow causes the hair to periodically rotate due to a drag torque $T(t)$ caused by viscous forces [7]. The system's response is governed by its moment of inertia J, torsional resistance R and torsional stiffness S:

$$J\frac{d^2\theta(t)}{dt^2} + R\frac{d\theta(t)}{dt} + S\theta(t) = T_0\cos(\omega t) \qquad (1)$$

In our MEMS hair flow sensory system, the torsional stiffness S is controlled using a DC-bias voltage on the sensor membrane electrodes (Fig. 3). By symmetrically supplying voltages to the electrodes of the sensor, the electrostatic transduction nature of the system is exploited to obtain ESS. To model the system's behavior under application of symmetric DC-bias voltages, we consider the electrostatically induced torque and stiffness which can be calculated from the first and second derivative of the energy in the capacitor with respect to θ respectively.
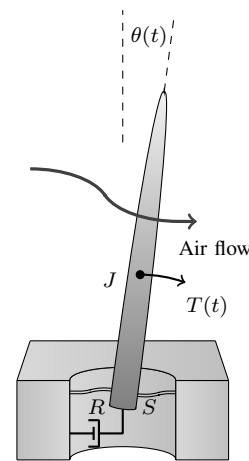

Fig. 2. Model of a flow sensing hair based on an inverted pendulum [5].

Due to the small angles θ encountered in practice and since the gap is much smaller than either the width w and length of the plates $2L$, the capacitor is treated as a parallel plate geometry (Fig. 4). The sensor operates in air, for which the relative electric permittivity ϵ_r is assumed to be equal to 1. Additionally, the silicon-nitride layers add some distance to the gap given by $t_{SiNi}/\epsilon_{r,SiNi}$ leading to an effective gap g_{eff}. The angle dependent capacitance $C(\theta)$ for the rotational sensor using the parallel plate approximation is given by:
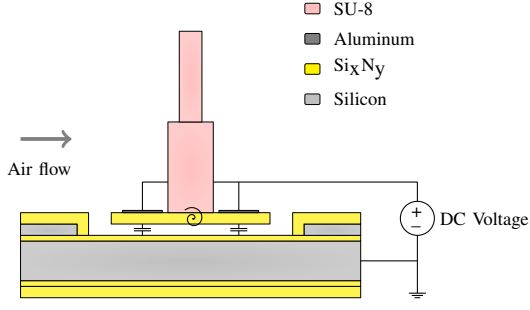
Fig. 3. Controlling the torsional stiffness by applying DC voltages to the sensor's capacitances.

$$C(\theta) = \int_{-L}^{L} \frac{\epsilon_0 w \cos(\theta)}{g_{\text{eff}} - x \sin(\theta)} dx \tag{2}$$

where x is the direction parallel to the plates and θ is the angle of rotation of the upper plate. The solution of this integral is given by:

$$C(\theta) = \epsilon_0 w \frac{\cos(\theta)}{\sin(\theta)} \ln\left(\frac{g_{\text{eff}} + L \sin(\theta)}{g_{\text{eff}} - L \sin(\theta)}\right) \tag{3}$$
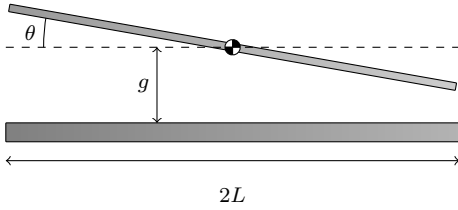

Fig. 4. Geometry of the angle-dependent rectangular capacitor.

Transduction principles are used to find the electrostatic spring softening by an angle-dependent and voltage-controlled capacitor. Since the total energy in the transducer, which is the sum of electrostatic energy in the capacitor and elastic energy in the spring, is given by

$$E(\theta, q) = \frac{1}{2} S_0 \theta^2 + \frac{1}{2} \frac{q^2}{C(\theta)} \tag{4}$$

the torque $T(\theta)$ is found from

$$\left.\frac{dE(\theta)}{d\theta}\right|_q = S_0\theta - \frac{1}{2}\frac{q^2}{C^2}\frac{dC(\theta)}{d\theta} = S_0\theta - \frac{1}{2}U_{\text{dc}}^2\frac{dC(\theta)}{d\theta} \tag{5}$$

and the effective stiffness from $dT(\theta)/d\theta = d^2E(\theta)/d\theta^2$. Hence on applying a DC-bias voltage U_{dc} the total torsional stiffness S becomes:

$$S = S_0 - \eta U_{\text{dc}}^2 \qquad \text{with} \qquad \eta = \frac{1}{2}\frac{d^2C}{d\theta^2} \tag{6}$$

These expressions state that the total torsional stiffness contains the intrinsic material-based stiffness S_0 and, under the small rotational angles normally encountered, a time-independent softening term dependent on the applied DC-bias voltage. For frequencies below the sensor's resonance

frequency the system shows a larger sensitivity. In addition, since the torsional stiffness S is reduced, also the resonance frequency ω_r of the system is affected:

$$\omega_r = \sqrt{\frac{S_0 - \eta U_{\text{dc}}^2}{J}} \tag{7}$$

Therefore, the sensor's sensitivity increases with applied DC-bias voltage, whereas the sensor's resonance frequency is simultaneously reduced.

B. Hair mechanics

The flow susceptible hair is subjected to an oscillatory flow $u(t)$ with a given amplitude U_0 and angular frequency ω. Assuming that the flow $u(t)$ is oscillating over a flat surface the no-slip boundary condition gives rise to the height y-dependent velocity profile [6]:

$$u(t) = U_0 \sin(\omega t) - U_0 e^{-\beta y} \sin(\omega t - \beta y) \tag{8}$$

where β is proportional to the reciprocal of the boundary layer thickness, with ν the kinematic viscosity ($\beta = \sqrt{\omega/(2\nu)}$).

Using trigonometric identities, this expression is written as a sinusoidal function with an amplitude U_y and phase shift ζ_y:

$$u_y(t) = U_y \sin(\omega t + \zeta_y) \tag{9}$$

where

$$U_y = U_0\sqrt{1 + e^{-2\beta y} - 2e^{-\beta y}\cos(\beta y)} \tag{10}$$

and

$$\zeta_y = \arctan\left(\frac{e^{-\beta y}\sin(\beta y)}{1 - e^{-\beta y}\cos(\beta y)}\right) \tag{11}$$

With the velocity profile known, the forces exerted on the hair are calculated by Stokes' mechanical impedance Z_S of an inverted pendulum in an oscillatory flow. Under the assumption of small angular displacements [7] the relationship between the flow velocity U and the drag force per unit length F can be expressed as:

$$Z_S = \frac{F}{U} = Z_{\text{SR}} + jZ_{\text{SX}} \tag{12}$$

where

$$Z_{\text{SR}} = 4\pi\mu_a G \qquad Z_{\text{SX}} = -\pi^2\mu_a G + \pi\rho_a\left(\frac{d}{2}\right)^2\omega \tag{13}$$

In these equations G, g and s are dimensionless parameters:

$$G = \frac{-g}{g^2 + (\pi/4)^2} \qquad g = \gamma + \ln(s) \qquad s = \frac{d}{4}\sqrt{\frac{\omega}{\nu}} = d\beta \tag{14}$$

where the dimensionless parameter $s << 1$ and d is the hair diameter. The dynamic drag force $F_t(t)$ can be expressed as:

$$F_t(t) = U_0|Z_S|\sin(\omega t + \eta_S) \tag{15}$$

where

$$|Z_\text{S}| = \sqrt{Z_\text{SR}^2 + Z_{SX}^2} \qquad \eta_\text{S} = \arctan\left(\frac{Z_\text{SX}}{Z_\text{SR}}\right) \qquad (16)$$

The absolute velocity profile of the oscillatory flow is given by (9), but to calculate the drag forces on the hair using Stokes's mechanical impedance, the relative velocity of the hair u_ry is required, where y is the position along the hair. Also, the resulting hair movement is assumed to be sinusoidal:

$$u_\text{ry}(t) = U_y \sin(\omega t + \zeta_\text{y}) - y\Theta_\text{m}\omega \cos\left(\omega t + \phi_\text{m}\right) \qquad (17)$$

Using Stokes's mechanical impedance, the resulting force per unit length on the flow susceptible hair is found:

$$F_\text{ty}(t) = |Z_\text{S}|\Big[U_y \sin(\omega t + \zeta_\text{y} + \eta_\text{S}) - y\Theta_\text{m}\omega \cos\left(\omega t + \phi_\text{m} + \eta_\text{S}\right)\Big] \qquad (18)$$

The torque $T(t)$ on the hair is calculated from the force per unit length $F(t)$ acting on the hair:

$$T(t) = \int_0^L F_\text{ty}(t,y)y\,dy \qquad (19)$$

Using Stokes' mechanical impedance and following [5], the angular deflection Θ_m is calculated:

$$\Theta_\text{m} = \frac{\sqrt{A^2 + B^2}}{\sqrt{\left[S - J\omega^2 - C\omega\right]^2 + \left[(R + D)\omega\right]^2}} \qquad (20)$$

where

$$A = \int_0^L |Z_S|U_y y \cos(\zeta_y + \eta_S)dy \quad C = \int_0^L |Z_S|y^2 \sin(\eta_S)dy$$
$$B = \int_0^L |Z_S|U_y y \sin(\zeta_y + \eta_S)dy \quad D = \int_0^L |Z_S|y^2 \cos(\eta_S)dy \qquad (21)$$

III. Experimental

A. Setup

Experiments are performed using the setup shown in figure 5. A waveform generator (Agilent 33220A-001) is used for generating a sinusoidal signal at a frequency f_a that is supplied to an amplifier. This amplifier drives a loudspeaker (Visaton WS 17 E) to generate the oscillating air flow at a frequency f_a. A wafer is glued on the loudspeaker cone to achieve a flow profile that can be well described by (very) near field theory [8].

Another voltage source (Delta Elektronika – Power Supply E 030–1) is used to supply the DC bias voltage to the top electrodes. The bottom electrode is grounded as is the measurement setup. The sensor rotational angle θ was derived from Laser Doppler Vibrometry using a Polytec MSA-400, since there is a simple factor between the measured membrane displacement and the hair rotational angle.
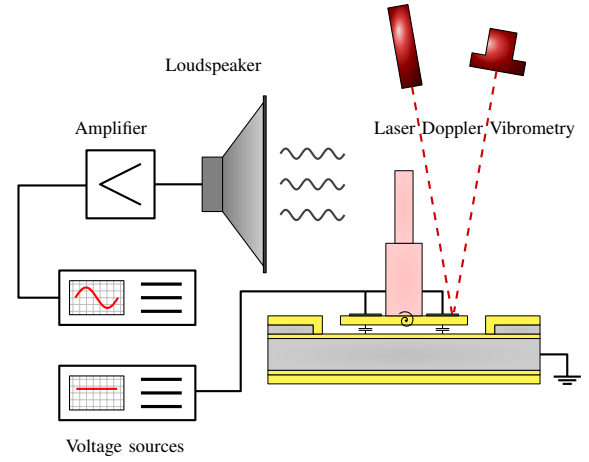

Fig. 5. Measurement setup for determining the membrane displacement of the hair flow sensor.

B. Mechanical transfer

First, the mechanical transfer of the hair sensory system was determined (Fig. 6). During this measurement, a voltage of 2.5 V was used, giving an increase in sensitivity of about 80% for frequencies within the sensor's bandwidth. Also lowering of the resonance frequency ω_r is observed (about 20%).
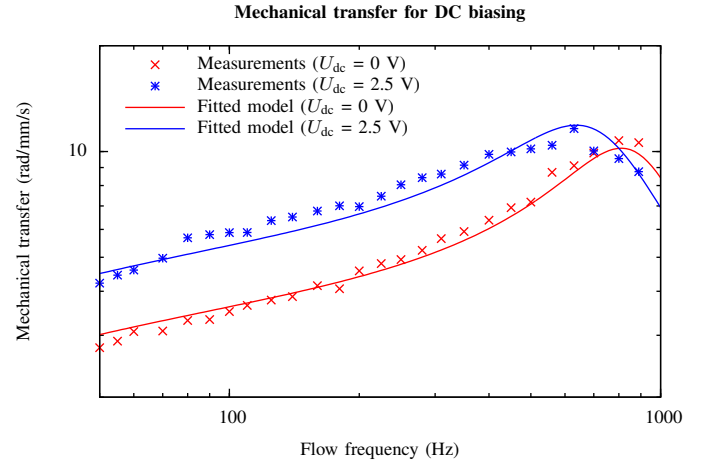

Fig. 6. Enhancing the mechanical transfer of the hair flow sensor by applying a DC voltage.

Further, the relationship between DC-bias voltage U_dc and its effect on the mechanical transfer of the system is measured (Fig. 7). For both frequencies of 100 Hz and 300 Hz a non-linear relationship is observed.

C. Threshold lowering

Next, the detection limit of the flow sensory system was measured with an without application of a DC-bias voltage for an harmonic flow of 110 Hz. Specifying the detection limit as being the flow-velocity amplitude at which the Signal-to-Noise Ratio (SNR) is equal to 1, our sensory system shows
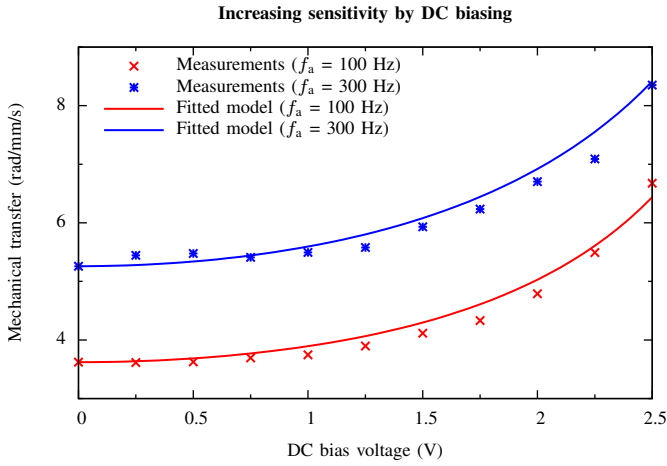
Fig. 7. Sensitivity increases nonlinearly with respect to the applied DC bias voltage.

an improvement of more than 30% (Fig. 8). The fitted model for the membrane displacement z is based upon the SNR:

$$z = \sqrt{(S_c U_0)^2 + N_c^2} \tag{22}$$

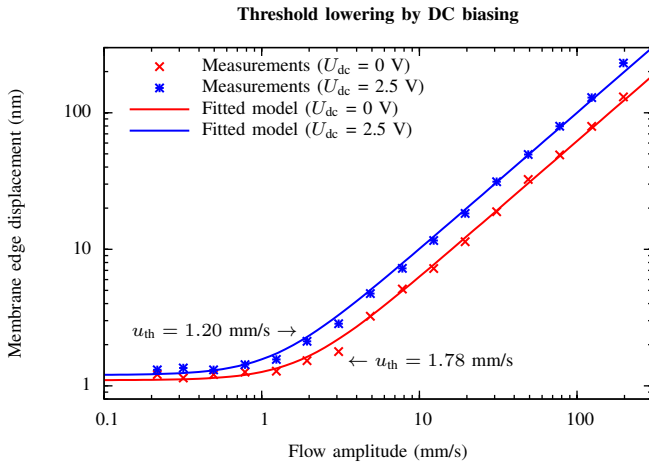where U_0 is the flow velocity amplitude, and S_c and N_c are fitting constants.

Fig. 8. Threshold lowering by DC biasing at 110 Hz, giving an improvement of more than 30% for $U_{dc} = 2.5$ V.

IV. DISCUSSION

Measurements for the mechanical transfer are in good agreement with modeling and it is shown clearly that DC-biasing leads to a larger sensitivity below the sensor's resonance frequency (Fig. 6). The resonance frequency of the system is also lowered, as predicted by (7). As a result, ESS can be used to adapt the sensor's performance to the environment by either adjusting it for a large bandwidth or a high sensitivity.

The non-linear relationship between the DC bias voltage U_{dc} and the torsional stiffness S is confirmed by measurements

(Fig. 7). Fitting the model from (20) and evaluating the constant η defined in (6), a value of $0.5 \cdot 10^{-9}$ Nm/(radV^2) is found, which is comparable to the calculated value of $0.58 \cdot 10^{-9}$ Nm/(radV^2) for a gap g of 1 μm.

Although a higher DC bias voltage results in an increased sensitivity, there exists a trade-off between increased sensitivity and stability, because of the pull-in effect — S becomes very small or negative.

Depending on the origin of the noise present in the sensory system, ESS can result in a lower sensory threshold and thus help to improve the detection limit of the sensor. Our current flow sensors have a detection limit of about 1 mm/s for oscillating air flows at about 100 Hz, but based on thermal noise calculations it is expected that this can be lowered significantly [9]. Our measurements show that ESS increases the detection limit of the sensor by increasing its sensitivity, although the noise floor itself is also slightly increased (Fig. 8). A possible explanation is the reduced capacitor gap g due to the sensor's limited vertical stiffness. As a consequence of an increased DC-bias voltage, the squeezed film damping is also increased and thus the thermal mechanical noise.

V. CONCLUSION

In conclusion, applying a DC-bias voltage to our biomimetic hair flow sensors gives both an increase in sensitivity for frequencies within the sensor's bandwidth and lowers the sensory threshold. Therefore, we can detect lower flow velocities by adapting our flow sensors using DC-bias voltages.

REFERENCES

[1] D. Avitabile, M. Homer, A. R. Champneys, J. C. Jackson and D. Robert, "Mathematical modelling of the active hearing process in mosquitoes", J. R. So. Interface, Vol. 7, pp. 105–122, 2010.
[2] M. A. Dijkstra, J. J. J. van Baar, R. J. Wiegerink, T. S. J. Lammerink, J. H. de Boer and G. J. M. Krijnen, "Artificial sensory hairs based on the flow sensitive receptor hairs of crickets", J. Micromech. Eng., Vol. 15, pp. S132–S138, 2005.
[3] C. M. Bruinink, R. K. Jaganatharaja, M. J. de Boer, J. W. Berenschot, M. L. Kolster, T. S. J. Lammerink, R. J. Wiegerink and G. J. M. Krijnen, "Advancements in technology and design of biomimetic flow-sensor arrays", *Proceedings, MEMS 2009 Conference, Sorrento, Italy*, January 25–29, 2009, pp. 152–155.
[4] J. Floris, N. Izadi, R.K. Jaganatharaja, R.J. Wiegerink, T.S.J. Lammerink and G.J.M. Krijnen, "Adaptation for frequency focusing and increased sensitivity in biomimetic flow sensors using electrostatic spring softening", Proceedings, Transducers 2007 Conference, Lyon, France, June 10–14, 2007, pp. 1267-1270.
[5] T. Shimozawa, T. Kumagai and Y. Baba, "Structural scaling and functional design of the cercal windreceptor hairs of cricket", J. of Comp. Physiol. A, Vol. 183, pp. 171–186, 1998.
[6] R. L. Panton, "Incompressible flow", Wiley, 1996.
[7] G. G. Stokes, "On the effect of the internal friction of fluids on the motion of pendulums", Trans. of the Cambr. Phil. Soc., Vol. 9, 8ff, 1851.
[8] H. E. de Bree, V. B. Svetovoy, R. Raangs and R. Visser, "The very near field: Theory, simulations and measurements of sound pressure and particle velocity", 11th Int. Congr. Snd. Vibr., 2004.
[9] A. M. K. Dagamseh and G. J. M. Krijnen, "Thermal noise estimation in bio-inspired hair flow sensor", Proceedings, 1st Int. Conf. on Nat. and Biomim. Mechanosens., Dresden, Germany, October 26–28 2009, 64.